

## Scintillator/WLS Fiber Readout with PSiPs

---

**Robert J. Wilson<sup>1</sup>, Yvan Caffari, David Warner, Eric Martin, Pablo Bauleo**

*Department of Physics, Colorado State University*

*Fort Collins, CO 80523, USA*

*E-mail: wilson@lamar.colostate.edu, ycaffari@lamar.colostate.edu*

We report on the use of two varieties of Pixelated Silicon Photosensors (PSiPs) as the readout for two scintillator/wavelength shifting fiber configurations. One configuration, a rectangular cross-section scintillator bar similar to that used in the MINOS experiment, is under consideration for the muon system of an International Linear Collider detector; the second, a triangular cross-section scintillator bar developed for the MINERvA experiment, is planned for use in the T2K experiment pi-zero detector subsystem. The PSiPs tested were the 400 pixel Multi-Pixel Photon Counter (MPPC) from Hamamatsu Photonics K.K. (HPK) and the 556 pixel Metal-Resistor-Semiconductor (MRS) from the Center of Perspective Technologies and Apparatus (CPTA). Data were collected in a 120 GeV test beam at Fermi National Accelerator Laboratory. We report also on a new high density photosensor from aPeak inc. able to read out sixty four close-packed 1.2 mm diameters fibers on a single chip.

*International workshop on new photon-detectors PD07  
Kobe University, Kobe, Japan  
27-29 June, 2007*

---

<sup>1</sup> Speaker and corresponding author.

## 1. Introduction

In the past five years the use of pixelated Geiger-mode avalanche photodiodes (GPDs) as photosensors for high energy physics applications has gone from an interesting idea to a true enabling technology that allows detector design options not possible with previous options. These devices are small, inexpensive, and insensitive to magnetic fields obviating the need to transport the light generated in scintillator-based detectors through long optical fibers. To avoid concerns over the use of proprietary terminology when referring to these devices, we have adopted the acronym PSiPs (pronounced “sipes”) as a generic term for all Pixelated Silicon Photosensors.

The results presented in this paper are the result of two research interests of the Colorado State University (CSU) group that have recently converged.

One is a long-term association with aPeak Inc. [1], a U.S. developer of silicon photosensors. The CSU group has advised aPeak on the development of a variety of GPD designs ranging from arrays of single UV photon sensitive pixel devices for Cerenkov applications, to single pixel and arrays of visible light sensors. aPeak received R&D funds from the US Small Business Administration Innovative Research (SBIR) program to develop these devices and then subcontracted with CSU to evaluate them for HEP applications. The CSU group also received funds from the Linear Collider R&D program to investigate the use of these devices to read out a Linear Collider Detector concept muon system based on the MINOS experiment scintillator bar with embedded Y-11 WLS fiber [2] [3].

More recently, the CSU group joined the Tokai-to-Kamioka (T2K) long baseline neutrino oscillation experiment in Japan. For this experiment, a detector is being built near the neutrino source to characterize the beam and to measure important background processes. The “Near Detector at 280 m (ND280)” [4] consists of several subsystems that use scintillator with embedded wavelength-shifting fiber as the detector medium. One of responsibilities of the CSU group is selection of a commercially available device and testing of the nearly 11,000 photosensors for the ND280 pi-zero detector subsystem.

In the first section of this paper, we present the results of bench tests of a new high-density device from aPeak that allows single-chip readout of 64 1-mm diameter fibers. In the second section we report on the use of two varieties of PSiPs as the readout for two scintillator/wavelength shifting fiber configurations under beam test conditions. One configuration, a rectangular cross-section scintillator bar similar to that used in the MINOS experiment, is under consideration for the muon system of an International Linear Collider detector; the second, a triangular cross-section scintillator bar developed for the MINERvA experiment, is planned for use in the T2K experiment pi-zero detector subsystem.

## 2. Bench Tests of aPeak Inc. Geiger-mode Photo-diodes (GPDs)

As part of a US Small Business Innovation Research (SBIR) Phase II award through the US Department of Energy [5], the CSU HEP group was contracted by aPeak Inc. to investigate the performance of their Geiger-mode Avalanche Photodiodes (GPDs) for typical HEP

applications. The CSU group assisted aPeak in securing this and previous SBIR awards that have allowed a university-industry partnership not otherwise possible.

Our initial tests of aPeak devices involved cosmic rays traversing a sample of scintillator used in the MINOS calorimeter system. This consists of a 41 mm x 10 mm rectangular cross section extruded scintillator bar, coated with a 0.25 mm TiO<sub>2</sub> reflective cap, with a groove cut down the center of one wide face to accommodate a 1.2 mm Kuraray Y11 wavelength-shifting (WLS) fiber. A scintillator hodoscope was used to trigger on approximately vertical cosmic rays (VCR) passing through the bar roughly 4 cm from the readout end of the bar. Charge spectra collected using EMI 911B photomultiplier tube (pmt) as the photosensor yields a distribution with a mean of 11 pC. We use this value to define a unit of 1 “VCR” as a reference point. There is no absolute calibration, but we estimate that 1 VCR deposits about 2 MeV in the bar and produces about 150 photons out of the Y11 fiber.

To enable faster investigation of GPD characteristics, the scintillator/fiber is replaced with an LED with an emission wavelength of 550 nm, which is well-matched to the peak of the Y11 WLS fiber output. To calibrate the LED intensity to 1 VCR, it is placed 80 cm away from the pmt which is covered by an opaque cap with a 1.0 mm hole through to the photocathode to emulate the active area of the GPD. In Figure 1 the blue histogram shows the pmt charge collected in a 180 ns gate for 1 VCR; overlaid on this is the pmt response to the LED energized by a pulse with 2.5 V amplitude and 14.5 ns wide. The central width of the LED distribution matches that of the cosmic distribution but lacks the high tail of cosmic ray sample – nonetheless it is adequate for the purpose of rapid testing of PSiP samples. The LED driving pulse parameters could be adjusted to shift the peak of the distribution over the range 0.2-13 VCR; how well these distributions correspond to shape and spectrum of true multiple VCRs is unknown.

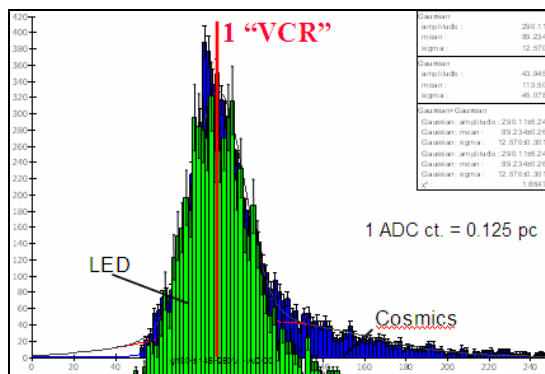


**Figure 1:** PMT spectrum for approximately vertical cosmic rays passing through MINOS scintillator/WLS (blue), overlaid with spectrum when a pulsed 550 nm LED replaces the bar as a light source.

**2.1 64-fiber Readout GPD**

A goal of aPeak has been to produce a high efficiency, high-density, compact, and low-cost WLS/fiber readout targeted primarily for *non-calorimetric* use such as a tracking system, where high efficiency per layer is the main consideration. In 2006, aPeak produced the first

POS(PD07)010

prototype of a single chip that could read out sixty-four 1.2-mm diameter fibers. Each individual sensor consists of a cluster of sixteen  $160 \times 160 \mu\text{m}^2$  GPDs on  $240 \mu\text{m}$  centers. The geometrical efficiency of this configuration is 0.36 for a 1.2 mm diameter fiber and 0.45 for a 1 mm fiber. A significant advantage of this design is a very low operating bias voltage of around 14 volts.

The output of each sensor is proportional to the number of GPDs hit. The small dynamic range of this configuration is of minimal use for calorimetric applications, but it may provide useful hit threshold tuning information.

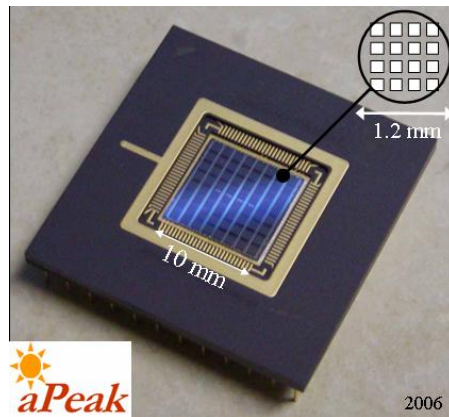


**Figure 2:** Compact readout for 64 1.2 mm WLS fibers from aPeak Inc.

With a bias voltage of -14.2 V and an LED pulse corresponding to 1 VCR, the average peak amplitude of the output of one pixel into a 10X linear amplifier was 300 mV at room temperature. The detection efficiency (DE) for this device is measured using two techniques. In the first method, the discriminated amplified signal was scaled in a counter and the DE calculated as  $(\text{Measured Rate} - \text{Dark Rate}) / \text{LED flash rate}$ . Figure 3 shows DE as a function of discriminator threshold for a range of LED intensity settings in units of VCRs. The dark count rate (DCR) is also plotted.

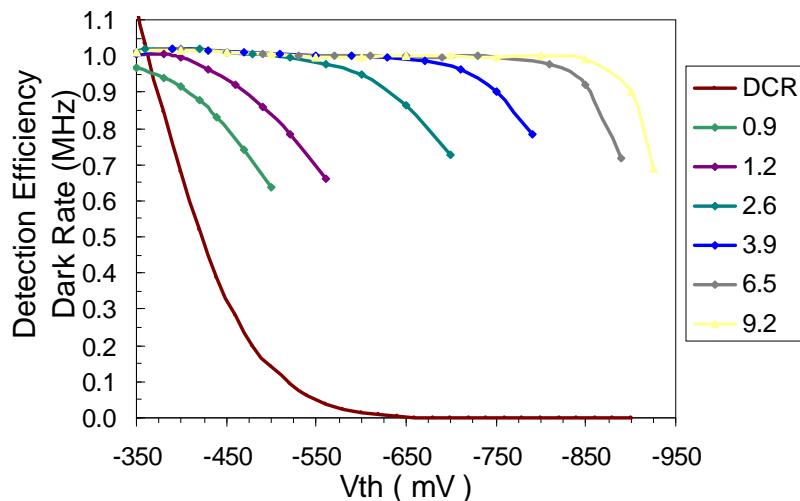


**Figure 3:** Dark Count Rate (DCR) and Detection Efficiency (DE) as a function of discriminator threshold for several LED intensities 0.9-9.2 expressed in units of vertical cosmic ray (VCR) equivalent. The GPD was operated with a bias voltage of -14.2V.

The significance of a high dark rate is application dependent. Typically, the trigger or data acquisition system requirements impose a practical limit and a high dark rate also leads to “accidental” coincidences that artificially enhance the detection efficiency described in the previous paragraph. The probability that a dark count falls within a gate width  $w$  is given by the product  $w \times \text{DCR}$ . For example, with a threshold of  $-400$  mV a signal equivalent to a single cosmic ray passing through the MINOS bar is detected with 95% DE, but with a gate width for these measurements of 500 ns, the corresponding dark rate of 0.6 MHz would produce a dark count within the gate 30% of the time. For a signal corresponding to the equivalent of two vertical cosmic rays a threshold that provides 95% detection efficiency has a 10% dark count probability.

A plot of the integrated charge from the GPD as a function of LED intensity is shown in Figure 4. Linearity of the 16 GPD cluster pixel response is evident up to 1.2 VCR, corresponding to about 10 photoelectrons; for higher light levels the measured charge saturates due to the small number of GPDs per cluster. There is a large pedestal offset that depends on the GPD bias voltage.

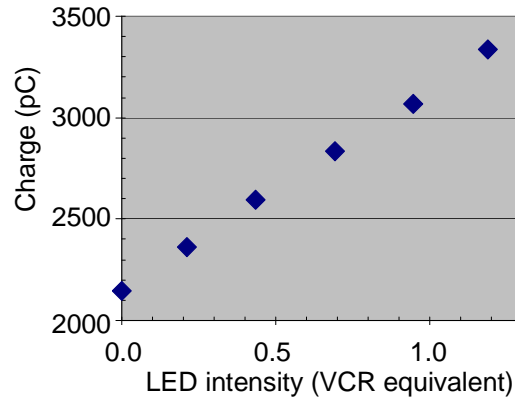


**Figure 4:** GPD response as a function of LED intensity in units of vertical cosmic ray (VCR) equivalent ( $-14.2$  V bias, room temperature).

From previous studies of aPeak prototypes based on the same processing technology, it was known that the devices operate more effectively with cooling to sub-zero temperatures. We performed a series of measurements using a computer-controlled Peltier refrigerator that allowed measurements at stabilized temperature from room temperature to  $-20^\circ\text{C}$ . At the lowest end of this range we observed well-separated photoelectron peaks in the charge spectrum for the first time (Figure 5). The device gain at a bias voltage of  $-13.4$  V determined from the separation between peaks is  $2.6 \times 10^6$ . Inspection of the dark spectrum indicates low crosstalk (few %). The detection efficiency from this data is calculated as the number of entries with measured charge above a particular value divided by the total number of triggers (LED flashes) in the sample. Figure 6 shows a set of measurements over a range of GPD bias voltages (13.3-13.7V) for a fixed LED intensity of 1VCR at  $-19^\circ\text{C}$ . The solid lines are the detection efficiency; the crosses of the same color are the corresponding dark rate. A DE of better than 98% is achieved with a corresponding dark spectrum value of less than 5%.

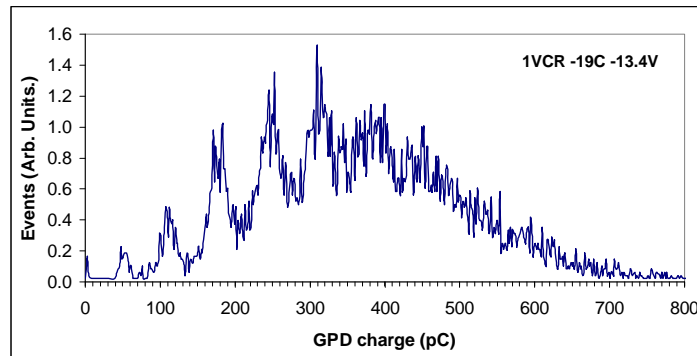


**Figure 5:** GPD (-13.4 V bias) response to low intensity LED pulses when cooled to -19°C.

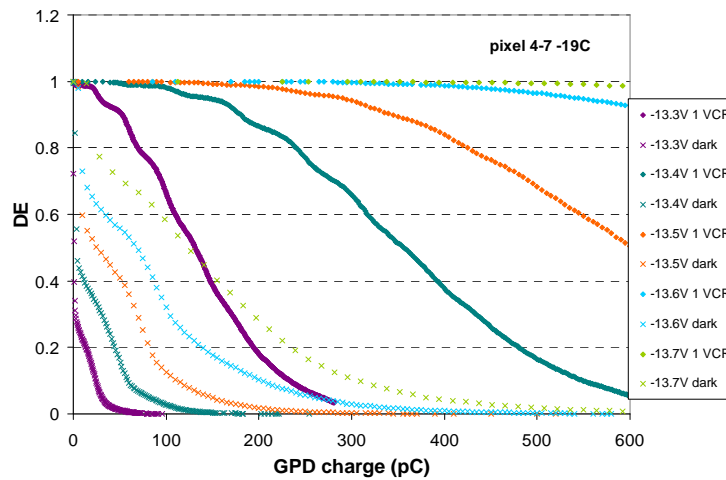


**Figure 6:** Detection Efficiency for 1VCR LED intensity (diamonds) and dark spectrum (crosses) as a function of integrated charge threshold for a range of bias voltages.

## 2.2 aPeak GPDs Summary

A new prototype high density device from aPeak Inc. targeted primarily at tracking or other threshold-type applications, allows readout of up to 64 1.2 mm WLS fibers in a footprint of 1 cm<sup>2</sup>. The device was fabricated using industry standard high-volume CMOS processing.

Linear response to low levels up to 10 p.e. was observed, consistent with the 16 GPD sub-structure of each pixel. Though of modest use for typical calorimetric applications, this feature may be useful for background reduction or data selection. At room temperature, detection efficiency of 95% is observed for signal level equivalent to 1 minimum ionizing track but the probability of dark noise hit is about 30%, doubling the signal level reduces the background probability to 10%. At temperatures below -10°C, well-separated multiple photoelectron peaks were observed at low light levels and high detection efficiency with low dark rates were demonstrated.

The most recent development at aPeak is the production of a new device designed for single fiber readout with 129 GPDs within the fiber footprint. Since it uses the same high-

volume process as the 64-readout chip single p.e. performance is not expected at room temperature, but preliminary measurements have demonstrated calorimetric behavior over a wider range of intensities.

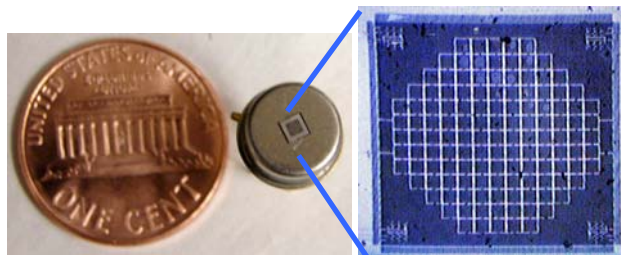


**Figure 7:** New aPeak Inc. 129 pixel GPD for single fiber readout.

### 3. FNAL Beam Test (Experiment T695)

An LED flasher used for lab studies of PSiPs (Section 2) allows rapid investigation of their basic characteristics, but it cannot replicate the Y11 output spectrum. It also does not map the position response of the scintillator/WLS, which is especially important in the triangular cross-section POD bars. Cosmic rays produce the minimum ionizing particle (MIP) response and energy scale but the low rate makes it difficult to test many devices and configurations. A low intensity beam of high energy particles addresses both of these issues. In March 2007 we were given access to such a beam at the new Fermi National Accelerator Lab Test Beam Facility (FTBF) [6] (just one month before our scheduled run, which proceeded well with only a few minor glitches).

The original motivation for the beam test was to investigate the potential use of PSiPs as a candidate photosensor for a scintillator-based Linear Collider Detector (LCD) muon system as part of a three-year study partially funded by the US Dept. of Energy Linear Collider R&D program. Initially only one scintillator/fiber geometry and one PSiP design was anticipated, ultimately this was expanded to include two geometries (rectangular and triangular cross-sections) and three PSiP designs were investigated. The report on data from two of the PSiPs (the third analysis is still in progress).

#### 3.1 Proton beam

The beam consisted of 120 GeV protons that arrived in a 1.58  $\mu\text{s}$  bunch train of eighty-four 18.87 ns buckets. With a single bunch in the main injector a train is delivered to FTBF every 12  $\mu\text{s}$  for a four second spill. The intensity was subject to some variation, but typically there were 40,000-60,000 protons distributed among the 333,000 trains in each spill. With this intensity we estimated there would be a single proton in about 85% of the triggers; this was confirmed by the energy spectra from our two scintillator trigger paddles positioned just upstream and downstream of the test box. The beam size was 3-4 mm RMS in the horizontal (which corresponding to the long dimension of our test bars) and 5-6 mm vertical (across the bars). Tracking information on the bunch particles was available, but it was not possible at that time to synchronize the data with our DAQ system so no precision track position information was available for the analysis.



### 3.2 Apparatus

The apparatus used to test the PSiPs under beam conditions consists of two rectangular cross section MINOS-style bars and three triangular cross section MINERvA /POD bars. The bars and photodetectors are housed in a light-tight 2.5m x 15 cm x 15 cm aluminum box. Figure 8 shows a photograph of the end box before (left) and after (right) the PSiPs (mounted in custom-designed machined plastic housings) are coupled to the 1.0 mm diameter WLS fibers for the MINOS bars and 1.2 mm diameter for the MINERvA bars. At the opposite end of the test bars (except MINOS 5) there is a photomultiplier tube (Hamamatsu R268,  $V_{op} = -1300$  V) used to monitor the bar response throughout the beam test.

Cooling loops were mounted to the outside of the aluminum box directly underneath the volume containing the PSiPs shown in Figure 8. Three thermocouples were mounted inside the PSiP volume – one on the aluminum wall, and two on the board holding the PSiP housings in position. During the beam test, the box was rotated 90° so the cooling loops were on a vertical face of the box. A temperature gradient of several degrees was measured in the photosensor volume such that the PSiPs on different bars were at a different temperature.

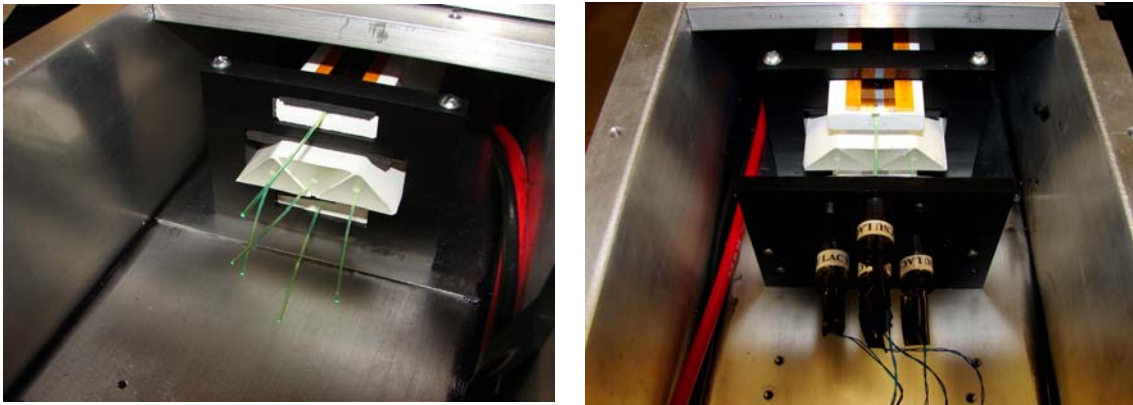


**Figure 8:** Rectangular MINOS bars above and below three triangular MINERvA/POD bars. The right-hand photograph shows installed PSiPs in custom optical connector housings. For the beam test, the box is rotated 90° so the beam first passes through the lower bar (MINOS 5), followed by the middle bars (MINERvA 2, 3, 4 from left to right) and upper bar (MINOS 1).

Altogether, fourteen different devices were tested: five 400 pixel Multi-Pixel Photon Counter (MPPC) model MPPC-11-T2K-5808 from Hamamatsu Photonics (HPK) with operating voltages of  $\sim 70$  V; four 556 pixel Metal Resistor Semiconductor (MRS) model MRS-1710 from the Center of Perspective Technologies and Apparatus (CPTA) with operating voltages in the range 44-48 V; and five 129 pixel GPDs from aPeak Inc. with operating voltages  $\sim 14$  V. Since analysis of the GPDs is not complete we report here only on the MPPC and MRS devices.

The front-end electronics consists of a passive filter close to the PSiP followed by RG158 signal cable to a 50 G<sub>v</sub> amplifier. The signal charge was measured with a charge-to-digital converter (CAEN V792N QDC) with a resolution of 0.1 pC per count mounted in a VME crate. Readout and control were provided by a LabView program running on a laptop computer. The



use of a small portable chiller unit allowed for data to be taken over temperature range from 12-20°C. In this paper we report on data taken with two configurations. In the first, the signal cables were 3.3 m long, the MPPC signal path included a 6dB attenuator, the integration gate was 400 ns, and the temperature range from 12-17°C. With this configuration it was not possible to resolve photoelectron peaks so a second set of data was taken with cable lengths reduced to 1 m, the attenuator was removed from the MPPC signal path and the integration gate reduced to 200 ns for the MPPC signals. The measured temperature was 17-20°C for these runs.

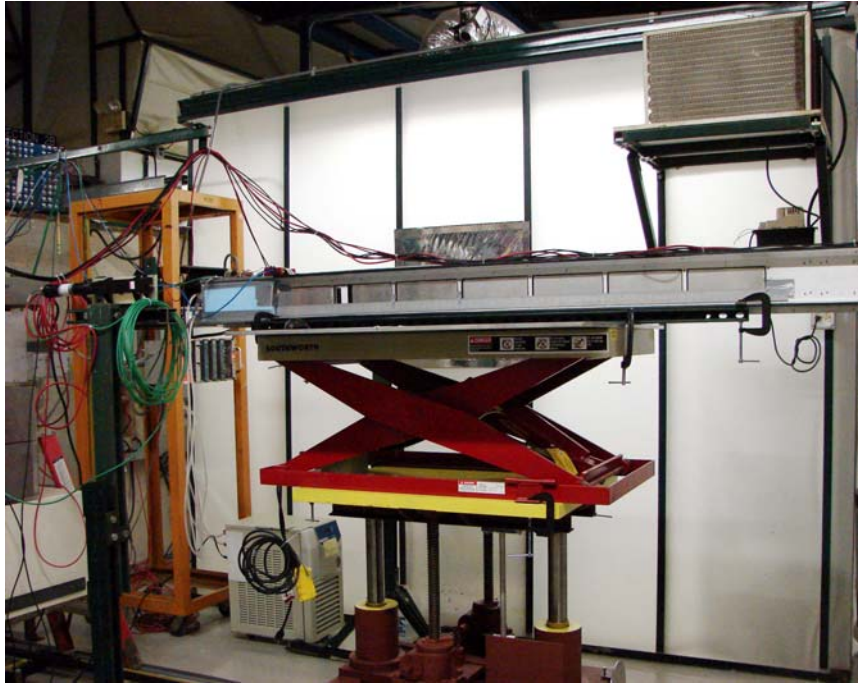


**Figure 9:** Test apparatus in the Fermilab test beam. The 2.5m x 15 cm x 15 cm aluminum support structure is mounted on a moveable table that can move horizontally and vertically under remote control.

### 3.3 Data Collection

Data were taken with the beam incident on the apparatus at three distances along the bars: 10 cm, 89 cm, and 175 cm. At each longitudinal position, data were taken at 3-5 vertical positions across the bars with 4 mm spacing. In the triangular cross section bars this provides a range of path lengths for the incident protons from a maximum of 15 mm at the apex down to a few mm at the edges. The rectangular bars have a uniform cross section of 10 mm except at the location of the groove holding the WLS. At each beam position, data were collected at a range of PSiP bias voltages.

The first runs collected data at all planned beam positions with a single photomultiplier tube<sup>1</sup> moved from one bar to the next to provide a single reference for comparison of signal levels from the PSiPs. The monitor pmts at the opposite end of each bar (except one) remained in place throughout the four day run period. Figure 10 shows the spectra from a run with the

<sup>1</sup> Electron Tubes 9111A,  $V_{op} = -950V$ , gain  $1.03 \times 10^7$

reference and monitoring pmts in place, along with the spectra from a later run at the same beam position but with an MPPC installed. The monitoring pmts have essentially the same mean value indicating that the light intensity generated in the bar was similar for both runs. After correcting for pedestal and gain, this allows a direct comparison of the signals measured by the reference pmt and the PSiPs on any bar.

To provide continuous monitoring of pedestals and dark count rates, the DAQ read out was triggered by a pulser running continuously at a rate of 100 Hz (“Beam Off” data) interspersed with beam triggers (“Beam On” data).

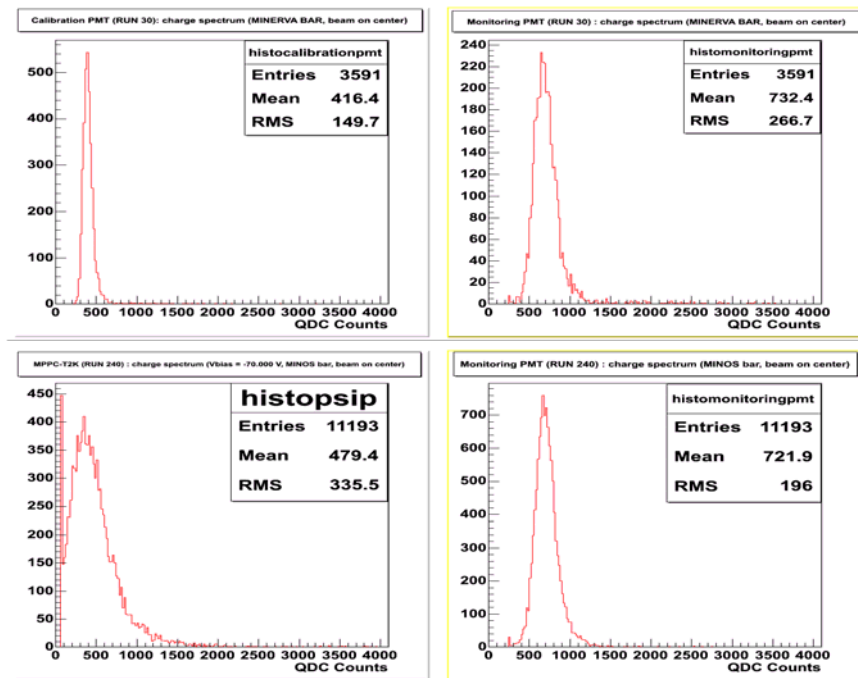


**Figure 10:** With the beam centered on a MINERvA bar (length and width), the top histograms show the spectrum recorded in a calibration pmt at one end and a monitoring pmt at the other (1 QDC count = 0.1 pC). The lower histograms show the spectrum for the same beam position but with the calibration pmt replaced by MPPC 51 operated with a bias of -70.0 V.

Data selection for analysis proceeded with a cut amplitude on the two hodoscope scintillators to select events with only a single proton within the gate. This corresponds to roughly 80% of the triggers, in general agreement with that expected estimated from the beam intensity and timing structure.

Figure 11 shows the spectra recorded from each MPPCs for a run in which the beam entered the bars 10 cm from the end closest to the PSiPs and such that the center of the beam passed midway between MINERvA bars 3 and 4. The large arrow on the schematics cross section indicates the beam direction, and its width represents the beam width to scale with the bar dimensions. The relatively broad beam means that the spectra from the triangular cross section bars include signals from a range of path lengths in the scintillator.

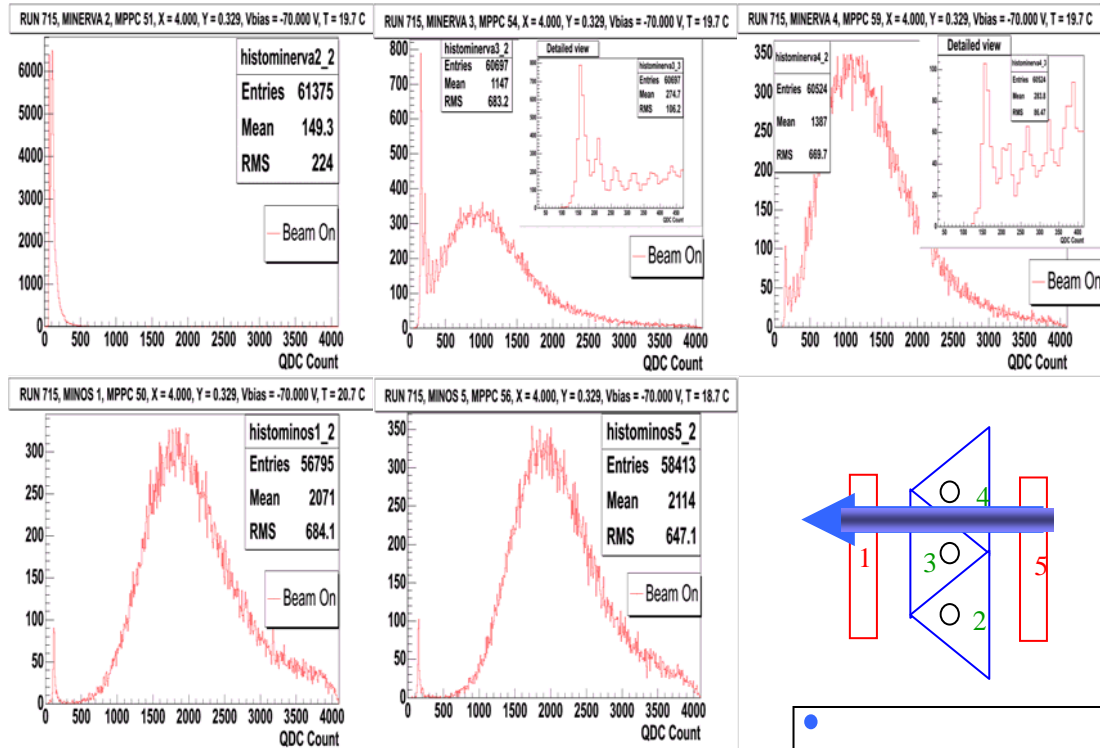


**Figure 11:** MPPC spectra recorded from each of test bars (MINERvA 2, 3, 4 across the top; MINOS 1 and 5 on the bottom) with the beam positioned as indicated in the diagram (1 QDC count = 0.1 pC). The arrow indicates the beam direction and the width corresponds roughly to the beam width, the beam passes about 4 cm from the end of the bar closest to the PSiPs. The MPPCs are all operated with a bias of -70.0 V at a temperature of about 20°C and an integration gate of 200 ns. The inset histograms provide a detailed view of the lower end of the spectrum.

Since no beam particles pass through the MINERvA 2 bar, the top left histogram shows just the pedestal and dark rate for that device. The bottom two histograms have almost identical spectra from the two rectangular cross section MINOS bars and the most probable value of these distributions provides the most direct measurement of the signal from a minimum ionizing particle. For these data the MPPC had a bias voltage of -70 V and were at a temperature of about 20°C. The two top left histograms are the spectra from the MINERvA bars directly in the beam. The lower pedestal and higher peak position indicates that the beam was shifted slight towards bar 4. The inset provides a closer view of the lower end of the spectra. Well-separated photoelectron peaks are easily identified and demonstrated one of the most attractive features of these devices. By identifying the lowest peak as the pedestal, the next as 1 p.e., then 2 p.e. etc., the absolute gain of the device can be determined directly from the beam data. The breakdown voltage for the device is determined from extrapolating the gain curve to zero gain.

The charge separation of the multiple photoelectron peaks in the signal, or dark spectrum, provides several measurements of the gain. Figure 12 show the gain as a function of bias voltage above breakdown (“over-voltage”) for the MPPCs tested. The gain dependence on bias voltage is linear and similar for all five devices and is consistent with the manufacturers’ data sheet to about 10%.

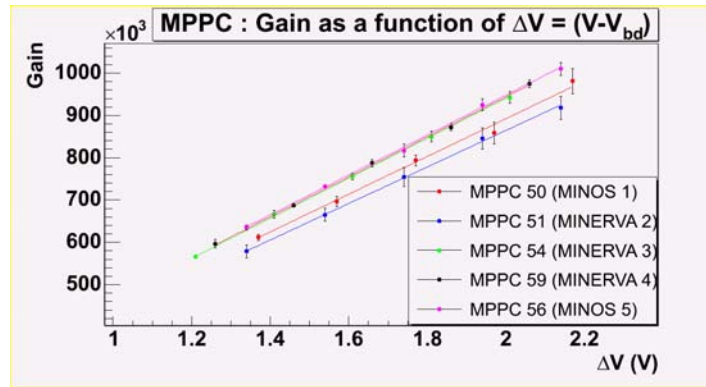


**Figure 12:** Charge gain of the five MPPCs as a function of the magnitude of the bias voltage above the device breakdown voltage.

Data for the same beam position with the MRS sensors produced similar distributions but the photoelectrons peaks were somewhat better defined for the lower intensity signals (Figure 13).

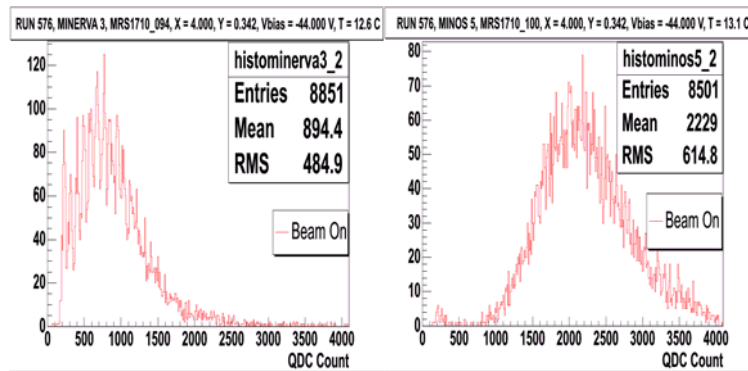


**Figure 13:** MRS spectra for the MINERVA 3 and MINOS 5 bars with beam position as with the previous figure. The devices are operated with a bias of -44.0 V at a temperature of about 13°C and an integration gate of 400 ns.

### 3.4 Dark/Beam-Off Spectrum

Inspection of the dark spectrum for the MPPC and MRS data highlights a significant difference in the tested devices. The MPPC spectrum on the left of Figure 14 has distinct photoelectron peaks (note the logarithmic scale), whereas the MRS spectrum on the right does not. Since the probability for observing uncorrelated dark counts from two pixels is very low, the relatively large number of multi-photoelectron peaks in the MPPC dark spectrum is an indicator of correlated additions to the charge spectrum. Originally, this was assumed to be pixel-to-pixel photon mediated crosstalk, but as reported elsewhere in this conference, it is now believed there is a substantial contribution from pulses in the same pixel that occur within the integration gate of the event – these are referred to as “after-pulses”.

If the position of the pedestal and 1 p.e. peaks can be identified, the dark count rate (DCR) can be determined from the data by dividing the number of entries above some threshold by the total number of entries multiplied by the gate width. Figure 15 shows the DCR for the five

MPPCs as a function of breakdown over-voltage for thresholds of 0.5 p.e. (left) and 1.5 p.e. (right), the integration gate is 200 ns. Compared to the manufacturer’s datasheet for rates at nominal operating voltages, the 0.5 p.e. rates measured here are lower by 10-30% and the 1.5 p.e. rate higher by a large factor of 5-7. We attribute this to a substantial crosstalk and/or after-pulsing as discussed in the next section.

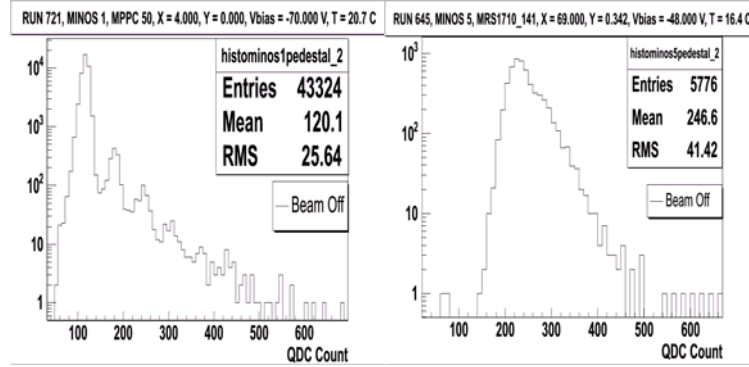


**Figure 14:** Dark spectra for the MPPC 50 and MRS 1710\_141 triggered by 100 Hz pulser during a run (“Beam Off” data is vetoed during the 4 second beam spill). The size of the multiple photoelectron peaks in the MPPC data indicates a high crosstalk and after-pulse rate.

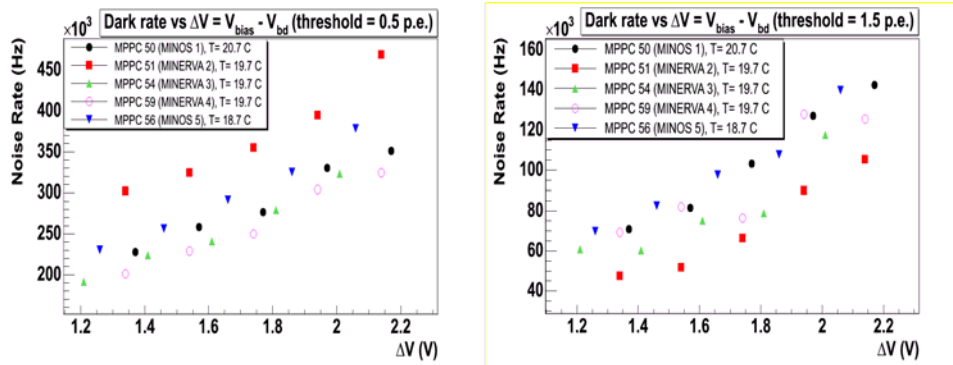


**Figure 15:** Dark rate of the five MPPCs as a function of the magnitude of the bias voltage above the device breakdown voltage (over-voltage) for a threshold of 0.5 p.e. (left) and 1.5 p.e. (right).

### 3.5 Crosstalk and After-Pulsing

As noted in the previous section, the dark count rates for the MPPC devices extracted from the “beam off” charge distribution deviate significantly from the expected values. Based on reports by others at this conference and direct inspection of signal traces in the lab, it seems likely that the relatively high bias voltages and long integration gates used for our data collection produced high crosstalk and after-pulsing contributions to the integrated signals. The result of these effects is to artificially increase the apparent signal above the true number of detected photoelectrons.

An estimate of the crosstalk and after-pulsing correction factor can be extracted from the dark spectrum by comparing the observed distribution with that expected if the data followed a



Poisson distribution. The Poisson probability distribution is of the form  $P(x; \lambda) = e^{-\lambda} \lambda^x / x!$ , where  $\lambda$  is the expected number of photoelectrons. Since  $\lambda = -\ln P(x=0)$ , we can estimate  $\lambda$  from the number of entries in the pedestal (0 p.e.) bins divided by the total number of entries. Note that the pedestal is independent of crosstalk or after-pulse effects. We use this to calculate the expected number of entries in the 1 p.e., 2 p.e., bins etc. The difference between the measured and expected number of entries is a measure of the deviation from a Poisson distribution due to crosstalk or after-pulses. This quantity was calculated for 20 consecutive runs and the mean of these measurements as a function of the breakdown over-voltage is shown in Figure 16. For four of the devices, this crosstalk factor is around 30% for lower voltages rising to 35-40% in the range measured. For one of the devices, the factor was a factor of two lower for unknown reasons.

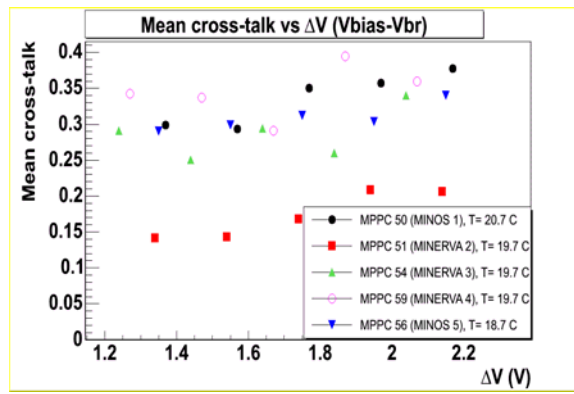


**Figure 16:** Mean crosstalk/after-pulse factor for MPPCs as a function of the breakdown over-voltage.

### 3.6 Attenuation

Though the initial primary reason for the beam test was to collect a large amount of data to measure device characteristics, it was of interest to the T2K/ND280 group to compare attenuation measurements in the MINERvA/P0D bars with assumptions made about the PSiP response in simulations used in the experiment design. To set the energy scale of interest for the ND280 pi-zero measurements, simulations show that for 98% of all neutrino interactions less than 19 MeV will be deposited in any single bar and for 30% of the events less than 1 MeV will be deposited. A minimizing ionizing particle deposits about 1.7 MeV/cm in plastic scintillator. The P0D simulation assumes a signal of 5.6 pe/MeV at the furthest point from the photosensor (~2.4 m), if the end of the fiber is mirrored. In the beam test configuration the far end of the fiber is coupled to a pmt and so is poorly reflecting, which reduces the expected signal by a factor of approximately 60%. With the proton beam centered on one of the P0D bars the P0D simulation predicts about 8 p.e. at the furthest end (175 cm) and 16 p.e. at the near end (10 cm).

For signal levels above a few photoelectrons, the most probable value of the signal is extracted by fitting the charge spectrum to the sum of a Gaussian and a Moyal<sup>2</sup> distribution. This value was converted to a number of photoelectrons using the gain extracted from the dark spectrum and correcting for the external amplification and passive attenuation (for cable configuration 1). Figure 17 shows the results for MPPC 54 and MRS1710\_94. The MPPC fit value was reduced by a factor of 0.7 to correct for the large after-pulse contribution to the integrated signal described in the previous section.

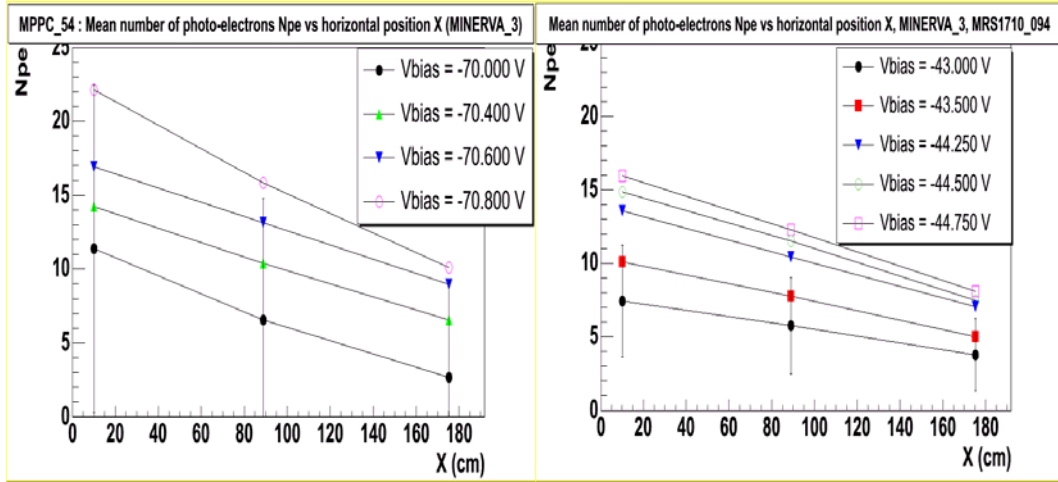


**Figure 17:** Attenuation along the MINERVA 3 bar measured by MPPC 54 and MRS 1710\_94 for a range of bias voltages. The number of photo-electrons is estimated from the most probable value of the charge distribution; the vertical bars on the lower curve indicates the width of the distributions. MPPC data includes a crosstalk/after-pulse factor of 0.7.

All device characteristics such as gain, photon detection efficiency, dark rate etc., are dependent on the bias voltage so the selection of optimum operating point is application dependent. In Figure 18 we present a comparison of the attenuation measurements for the MPPC, MRS and reference pmt, where the PSiP parameters are chosen to meet the ND280 front end electronics requirements for gain and dark rate<sup>3</sup>. The measured MPPC values at the near and far ends of the bar are similar to those assumed for the POD simulation; however, the large crosstalk/after-pulse correction is of concern. The lower noise ND280 electronics should allow operation at lower over-voltage ( $\sim 1$  V) and this should reduce the magnitude of the effect to acceptable levels (see papers by Vacheret and Retiere at this conference).

<sup>2</sup> The Moyal function  $M(x) = A \exp(-((x - \bar{x})/\sigma + e^{-(x-\bar{x})/\sigma})/2)$  represents a simple analytic approximation of the detector response to a minimum ionizing particle passing through the detector.

<sup>3</sup> MPPC 54 with  $V_{op} = -70.4V$ ,  $V_{op} - V_{br} = 1.68V$ ,  $gain = 8.7 \times 10^5$  (with these operating conditions the cross talk factor is  $\sim 35\%$ ); and MRS 111 with  $V_{op} = -42.5V$ ,  $V_{op} - V_{br} = 2.2V$ ,  $gain = 7.4 \times 10^5$  (crosstalk factor is assumed to be small)



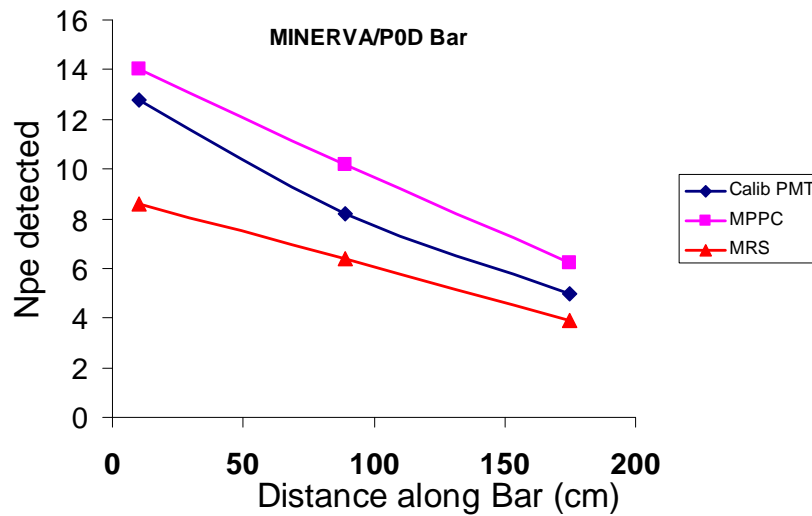


**Figure 18:** Attenuation along a MINERvA bar corrected for crosstalk/after-pulsing for MPPC (squares), MRS (triangles) and PMT (circles) for MPPC and MRS operating voltages that meet the T2K/ND280 electronics requirements for gain and dark rate.

### Acknowledgements

We would like to thank the staff of the Fermilab Test Beam Facility, particularly Erik Ramberg, for their valuable assistance during the beam test, and S. Vasile and staff at aPeak Inc. for their efforts to produce new photosensors for HEP applications.

### References

- [1] aPeak Inc., 63 Albert Road, Newton, MA 02466. Tel: (617) 964-1709 Fax: (617) 964-1709. Email: info@apeakinc.com. Web: <http://www.apeakinc.com>
- [2] P. Adamson et al., *The MINOS Calorimeter System*, IEEE Trans. Nuc. Sci., Volume 49, Issue 3, Oct. 2003 Page(s): 861 - 863
- [3] A. Pla-Dalmau, A.D. Bross, V.V. Rykalin *Extruding plastic scintillator at Fermilab*, IEEE Nucl. Sci. Symp. Conf. Rec., 2003, Vol. 1, Issue , Oct. 2003 Page(s): 102 - 104
- [4] <http://www.nd280.org>
- [5] US Department of Energy, <http://www.sc.doe.gov/sbir>
- [6] Fermilab Meson Test Beam Facility, <http://www-ppd.fnal.gov/MTBF-w/>. Contact: Erik Ramberg ([ramberg@fnal.gov](mailto:ramberg@fnal.gov)) X5731, MS 231.